**Supplementary Materials**

# Mildly oxidized and phenol-enriched carbon nanotubes as efficient and selective electrocatalysts for the 2e$^-$ oxygen reduction reaction

**Giulia Tuci[1,*], Marco Bonechi[2], Andrea Rossin[1], Enrico Berretti[1], Matteo Ceppatelli[1,3], Lorenzo Poggini[1,2], Massimo Innocenti[2], Giuliano Giambastiani[1,2,*]**

[1]Institute of Chemistry of OrganoMetallic Compounds, ICCOM-CNR, Sesto Fiorentino 50019, Florence, Italy.

[2]Department of Chemistry "U. Schiff" - DICUS - and INSTM Research Unit, University of Florence, Sesto Fiorentino 50019, Florence, Italy.

[3]LENS, European Laboratory for Non-linear Spectroscopy, Sesto Fiorentino 50019, Florence, Italy.

[*]**Correspondence to:** Dr. Giulia Tuci, Institute of Chemistry of OrganoMetallic Compounds, ICCOM-CNR, Via Madonna del Piano 10, Sesto Fiorentino 50019, Florence, Italy. E-mail: giulia.tuci@iccom.cnr.it; Prof. Giuliano Giambastiani, Department of Chemistry "U. Schiff" - DICUS - and INSTM Research Unit, University of Florence, Via della Lastruccia 3-13, Sesto Fiorentino 50019, Florence, Italy. E-mail: giuliano.giambastiani@unifi.it

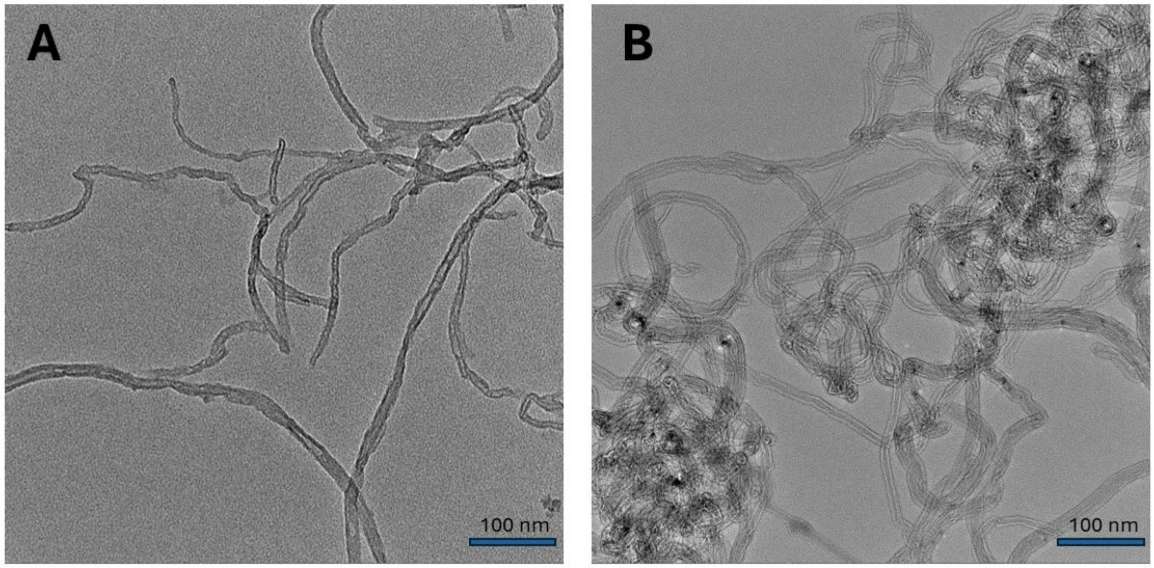


**Supplementary Figure 1.** TEM images recorded on (A) MW-ox$^{RT}$ (**1**) and (B) MW-ox$^{HT}$ (**2**).

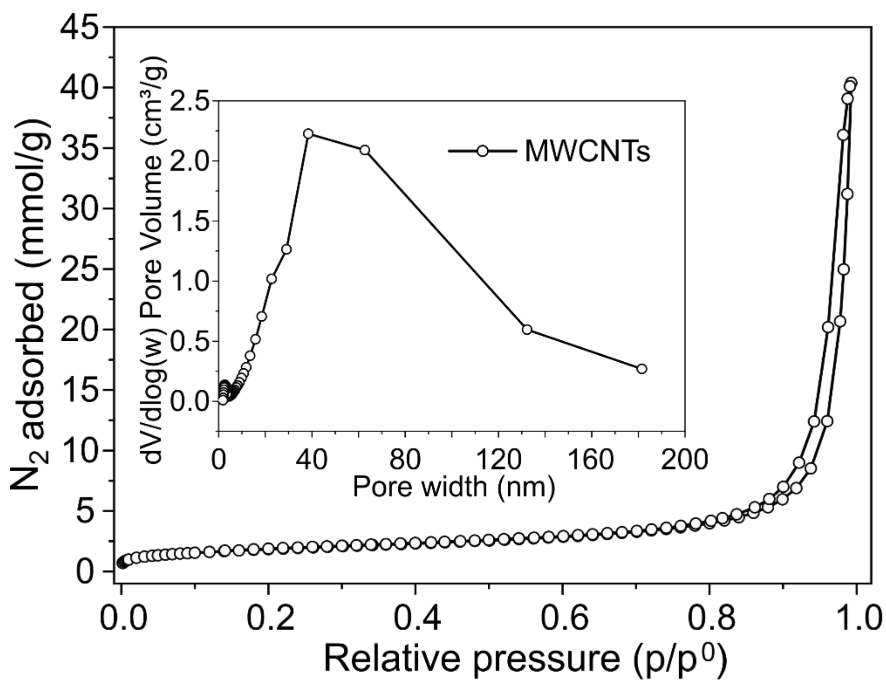


**Supplementary Figure 2.** $N_2$ adsorption-desorption isothermal curves conducted at 77 K for pristine MWCNTs along with their corresponding pore size distribution (inset).

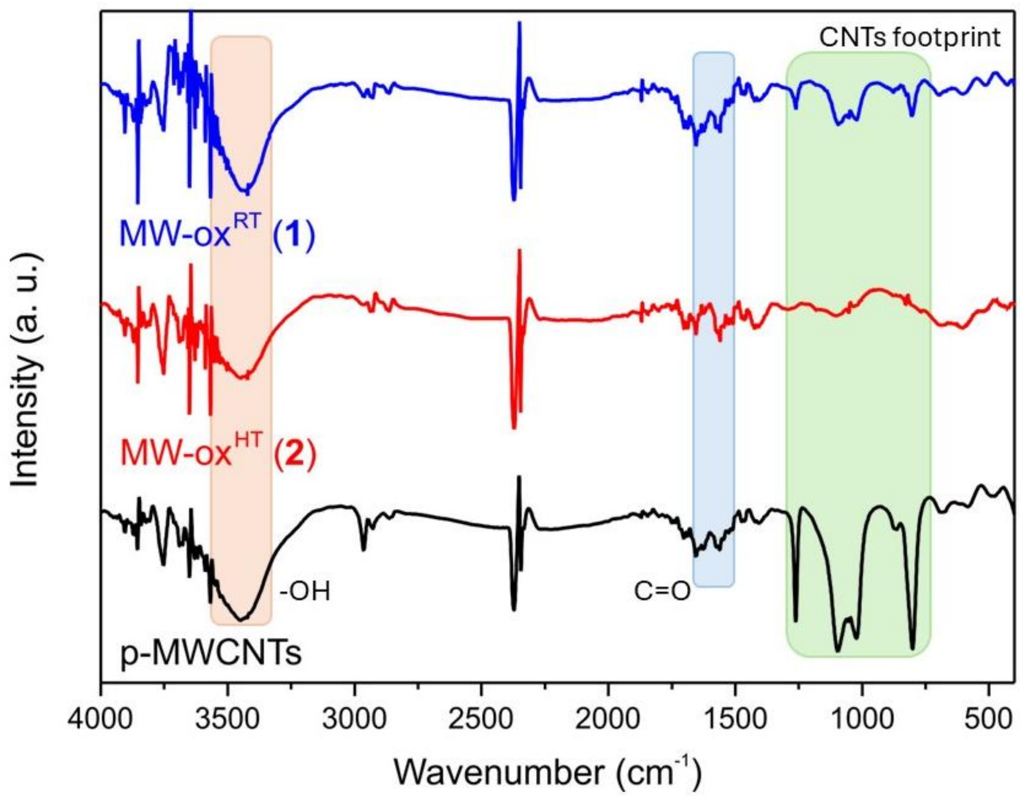


**Supplementary Figure 3.** FT-IR spectra of p-MWCNTs, MW-ox$^{RT}$ (**1**) and MW-ox$^{HT}$(**2**).

**Supplementary Table 1. Elemental analyses (EA) and semi-quantitative XPS analyses conducted on MW-ox$^{RT}$ (1) and MW-ox$^{HT}$(2).**

| | EA[a] | | XPS | | | |
|---|---|---|---|---|---|---|
| | C wt.% | H wt.% | O at.%[b] (wt.%) [c] | carboxylic groups (%)[d] | carbonyl groups (%)[d] | Phenolic groups (%)[d] |
| MW-ox$^{RT}$ (**1**) | 64.1 | 2.2 | 27.6[e] (33.7) | 52 | 36 | 12 |
| MW-ox$^{HT}$(**2**) | 76.5 | 0.9 | 19.2 (24.1) | 37 | 37 | 26 |

[a]average values calculated over three independent runs. [b] estimated from high resolution O 1*s* XPS signal. [c] calculated wt.% from XPS at.% data. [d] relative % calculated from fitting of high resolution 1*s* XPS signals. [e] 29.3 O at. % if adventitious water is taken into consideration.

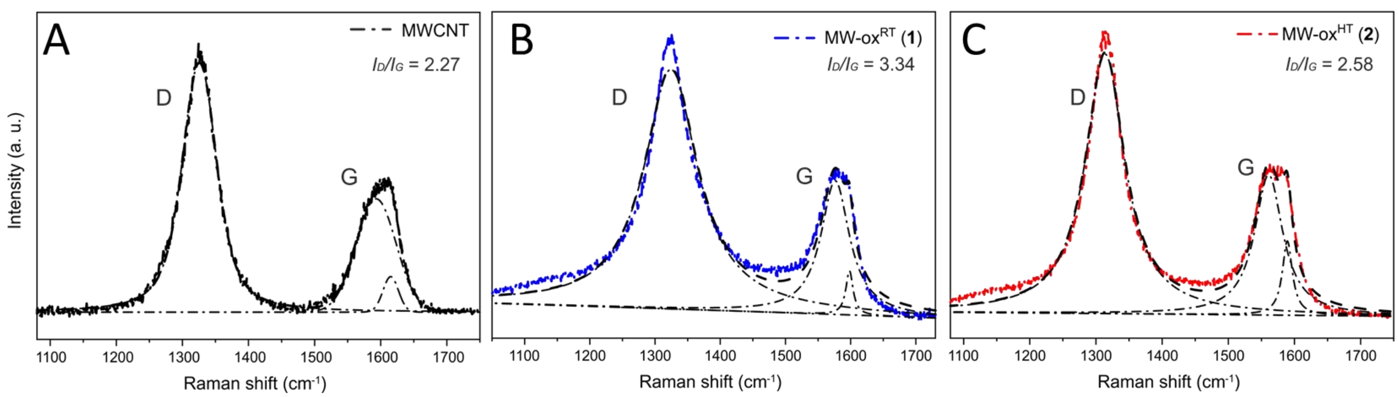


**Supplementary Figure 4.** Raman spectra of pristine MWCNTs (A) and oxidized samples **1** (B) and **2** (C) along with their relative fitting. $I_D/I_G$ ratio is 2.27, 3.34 and 2.58 for MWCNTs, MW-ox$^{RT}$ (**1**) and MW-ox$^{HT}$(**2**), respectively.

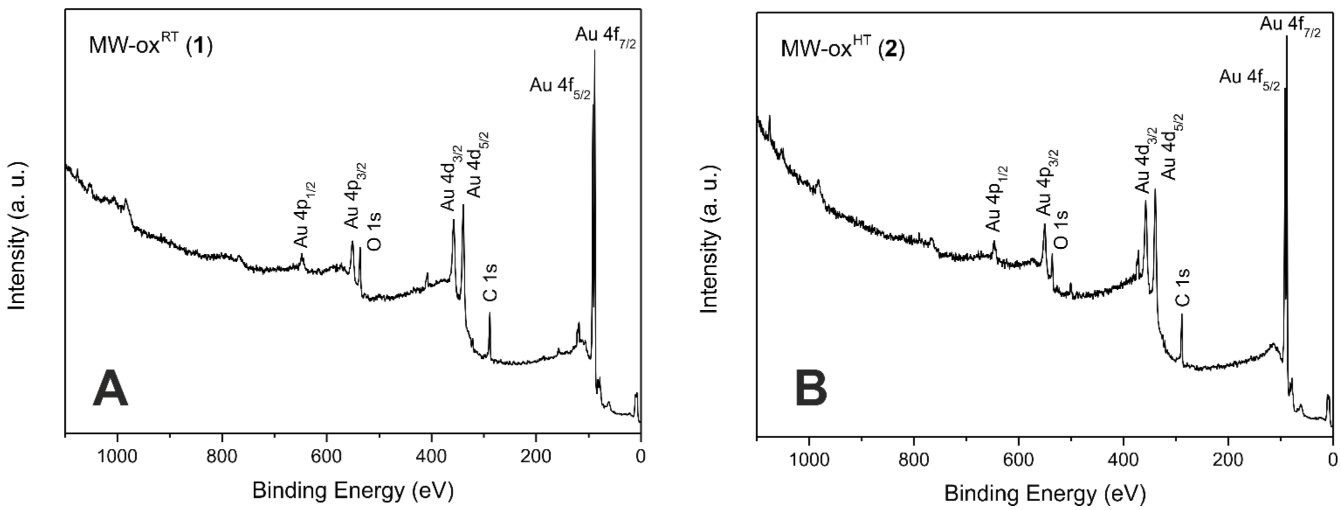


**Supplementary Figure 5.** XPS survey spectra of (A) MW-ox$^{RT}$ (**1**) and (B) MW-ox$^{HT}$(**2**).

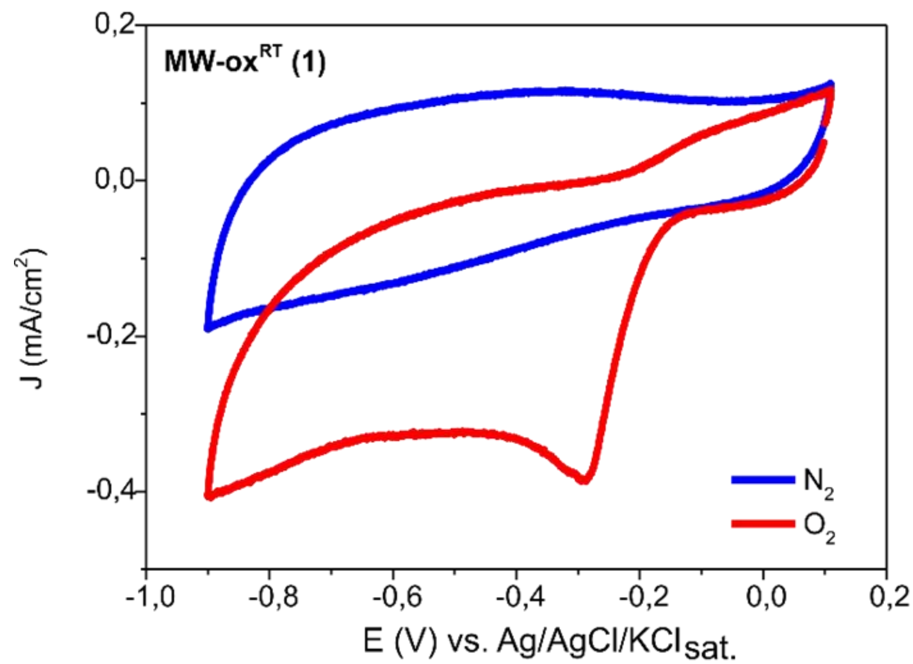


**Supplementary Figure 6.** Cyclic voltammetries (CV) acquired in $N_2$ and $O_2$ saturated KOH 0.1 M solution for MW-ox$^{RT}$ (**1**) at 10 mV/s in the +0.1 ÷ -0.9 V *vs*. Ag/AgCl/KCl$_{sat.}$ potential range.

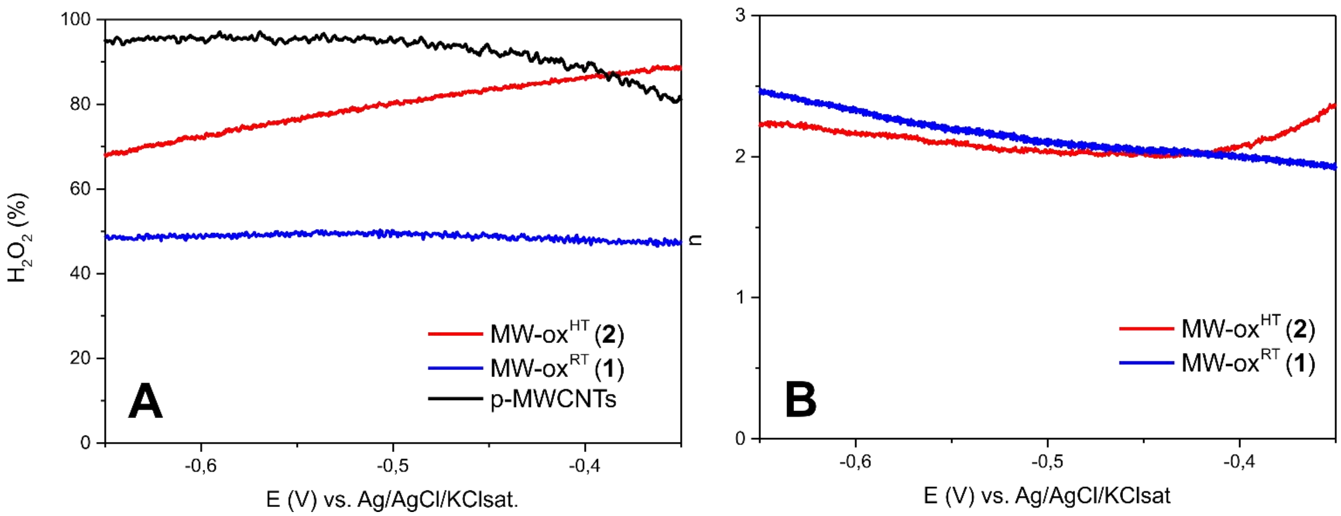


**Supplementary Figure 7.** (A) $H_2O_2$ % values as obtained from ring current values and (B) number of electrons exchanged *per* $O_2$ molecule (n) as obtained from K-L equation in the -0.65 ÷ -0.35 V potential range.

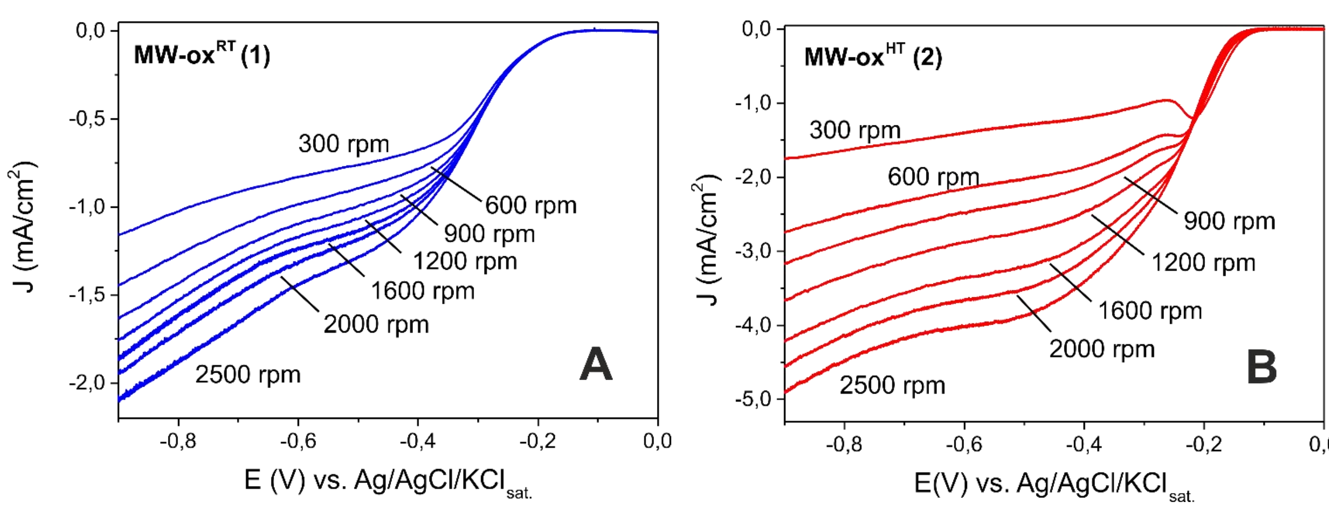


**Supplementary Figure 8.** LSV curves for (A) MW-ox$^{RT}$ (**1**) and (B) MW-ox$^{HT}$ (**2**) registered at 10 mV/s at variable electrode spin rates (300 - 2500 rpm).

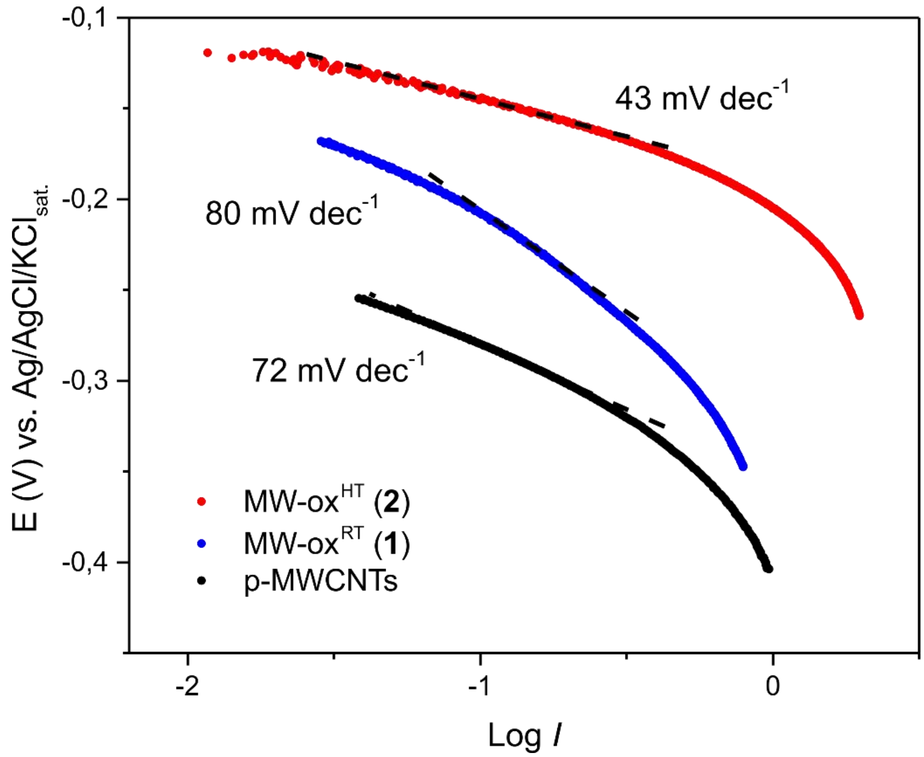


**Supplementary Figure 9.** Tafel plots obtained from LSV registered at 1600 rpm for p-MWCNTs, MW-ox$^{RT}$ (**1**) and MW-ox$^{HT}$ (**2**).

**Supplementary Table 2. Comparison of MW-ox$^{HT}$ (2) performance with the more representative O-decorated carbon-based materials from literature**

| Sample | $E_{ON}$ (V)[a] | $E_{1/2}$ (V)[a] | $H_2O_2$ (%) | Ref. |
|---|---|---|---|---|
| MW-ox$^{HT}$ (**2**) | **-0.14** | **-0.25** | **85** | This work |
| O-CNTs | -0.22 | -0.29 | 90 | [1] |
| *F*-mrGO | -0.19 | -0.32 | >99 | [2] |
| *o*-GOMC-1 | -0.16 | -0.29 | 93 | [3] |
| aCB | -0.15 | -0.23 | 94 | [4] |
| CB600 | -0.14 | -0.28 | 56 | [5] |
| $rGO_{KOH}$ | -0.16 | -0.30 | >99 | [6] |
| $GNP_{C=O}$ | -0.15 | -0.21 | 90 | [7] |
| NT-3DFG | -0.18 | -0.33 | 94 | [8] |
| MCHS-9:1 | -0.14 | -0.22 | 56 | [9] |
| HCNFs | -0.12 | -0.27 | 97 | [10] |
| O-GOMC | -0.16 | -0.24 | 90 | [11] |
| $OCNS_{900}$ | -0.19 | -0.21 | 90 | [12] |
| AC-$CO_2$B | -0.14 | -0.25 | 90 | [13] |
| CQD | -0.14 | -0.30 | 97 | [14] |
| MW/$C_6H_4OH$ | -0.15 | -0.29 | 79 | [15] |
| AQ-CNT-2 | -0.19 | -0.33 | 80 | [16] |
| C-O-12h | -0.19 | -0.26 | 85 | [17] |
| o-CNT 8 | -0.17 | -0.25 | 97 | [18] |

[a] Potential values *vs*. Ag/AgCl/$KCl_{sat}$

## REFERENCES


1. Lu Z, Chen G, Siahrostami S, et al., High-efficiency oxygen reduction to hydrogen peroxide catalysed by oxidized carbon materials. *Nat. Catal.* 2018; *1*: 156-62. DOI: 10.1038/s41929-017-0017-x
2. Kim HW, Ross MB, Kornienko N, et al., Efficient hydrogen peroxide generation using reduced graphene oxide-based oxygen reduction electrocatalysts. *Nat. Catal.* 2018; *1*: 282-90. DOI: 10.1038/s41929-018-0044-2
3. Sa YJ, Kim JH, Joo SH, Active Edge-Site-Rich Carbon Nanocatalysts with Enhanced ElectronTransfer for Efficient Electrochemical Hydrogen Peroxide Production. *Angew. Chem. Int. Ed.* 2019; *58*: 1100-5. DOI: 10.1002/anie.201812435
4. Wang W, Hu Y, Liu Y, Zheng Z, Chen S, Self-Powered and Highly Efficient Production of $H_2O_2$ through a Zn-Air Battery with Oxygenated Carbon Electrocatalyst. *ACS Appl. Mater. Interfaces* 2018; *10*: 31855-9. DOI: 10.1021/acsami.8b11703
5. Zhang H, Li Y, Zhao Y, Li G, Zhang F, Carbon Black Oxidized by Air Calcination for Enhanced $H_2O_2$ Generation and Effective Organics Degradation. *ACS Appl. Mater. Interfaces* 2019; *11*: 27846-53. DOI: 10.1021/acsami.9b07765
6. Zhu J, Xiao X, Zheng K, et al., KOH-treated reduced graphene oxide: 100% selectivity for $H_2O_2$ electroproduction. *Carbon* 2019; *153*: 6-11. Doi: 10.1016/j.carbon.2019.07.009
7. Han G-F, Li F, Zou W, et al., Building and identifying highly active oxygenated groups in carbon materials for oxygen reduction to $H_2O_2$. *Nat. Commun.* 2020; *11*: 2209. DOI: 10.1038/s41467-020-15782-z
8. San Roman D, Krishnamurthy D, Garg R, et al., Engineering Three-Dimensional (3D) Out-of-Plane Graphene Edge Sites for Highly Selective Two-Electron Oxygen Reduction Electrocatalysis. *ACS Catal.* 2020: 1993-2008.
9. Pang Y, Wang K, Xie H, Sun Y, Titirici M-M, Chai G-L, Mesoporous Carbon Hollow Spheres as Efficient Electrocatalysts for Oxygen Reduction to Hydrogen Peroxide in Neutral Electrolytes. *ACS Catal.* 2020; *10*: 7434-42. DOI: 10.1021/acscatal.0c00584
10. Dong K, Liang J, Wang Y, et al., Honeycomb Carbon Nanofibers: A Superhydrophilic $O_2$-Entrapping Electrocatalyst Enables Ultrahigh Mass Activity for the Two-Electron Oxygen Reduction Reaction. *Angew. Chem. Int. Ed.* 2021; *60*: 10583-7. DOI: 10.1002/anie.202101880
11. Lim JS, Kim HJ, Woo J, et al., Designing highly active nanoporous carbon $H_2O_2$ production electrocatalysts through active site identification. *Chem* 2021; *7*: 3114-30. DOI: 10.1016/j.chempr.2021.08.007

12. Chen S, Luo T, Chen K, et al., Chemical Identification of Catalytically Active Sites on Oxygen-doped Carbon Nanosheet to Decipher the High Activity for Electro-synthesis Hydrogen Peroxide. *Angew. Chem. Int. Ed.* 2021; *60*: 16607-14. DOI: 10.1002/anie.202104480

13. Sun F, Yang C, Qu Z, et al., Inexpensive activated coke electrocatalyst for high-efficiency hydrogen peroxide production: Coupling effects of amorphous carbon cluster and oxygen dopant. *Appl. Catal. B: Environ.* 2021; *286*: 119860. DOI: 10.1016/j.apcatb.2020.119860

14. Guo Y, Zhang R, Zhang S, et al., Ultrahigh oxygen-doped carbon quantum dots for highly efficient $H_2O_2$ production via two-electron electrochemical oxygen reduction. *Energy Environ. Sci.* 2022; *15*: 4167-74. DOI: 10.1039/d2ee01797k

15. Tuci G, Rossin A, Zhang X, et al., Metal-Free Electrocatalysts for the Selective 2e$^-$ Oxygen Reduction Reaction: A Never-Ending Story? *Chem. Eur. J.* 2023; *29*: e202301036. DOI: 10.1002/chem.202301036

16. Lee J, Lee Y, Lim JS, et al., Discriminating active sites for the electrochemical synthesis of $H_2O_2$ by molecular functionalisation of carbon nanotubes. *Nanoscale* 2023; *15*: 195-203. DOI: 10.1039/d2nr04652k

17. Xing Z, Shi K, Parsons ZS, Feng X, Interplay of Active Sites and Microenvironment in High-RateElectrosynthesis of $H_2O_2$ on Doped Carbon. *ACS Catal.* 2023; *13*: 2780-9. DOI: 10.1021/acscatal.2c05639

18. She F, Guo Z, Liu F, et al., Curvature-Dependent Electrochemical Hydrogen Peroxide SynthesisPerformance of Oxidized Carbon Nanotubes. *ACS Catal.* 2024; *14*: 10928-38. DOI: 10.1021/acscatal.4c01637